INVESTIGATION OF OPALS ON MARS USING CRISM DATA AND TERRESTRIAL ANALOGS.

M. Pineau[1], L. Le Deit[1], B. Rondeau[1], B. Chauviré[2], J. Carter[3] and N. Mangold[1] ; [1]LPG-Nantes, University of Nantes, France (Maxime.Pineau@univ-nantes.fr), [2]ISTerre, University Grenoble-Alpes, France, [3]IAS, Orsay, France.

Introduction: Over the last fifteen years, orbital studies of the Martian surface have shown numerous mineralogical evidences of water-rock interactions using the VNIR imaging spectrometers OMEGA and CRISM [1, 2]. However, climatic and environmental conditions prevailing during Early Mars remain under debate.

Several minerals, such as opal (hydrated amorphous silica) can form either at low temperature at/near the surface by supergene alteration (suggesting surface-atmosphere interactions) or at higher temperatures by hydrothermal alteration and do not require an open system to form. As opals have been detected across numerous regions [1, 2], they can provide constraints on the paleo-environmental conditions on Mars.

Previous studies based on the spectral analysis in the NIR signature of opals have shown that spectral criteria can be defined for discriminating different silica phases [3, 4]. Band shape measurements provide constraints on the formation processes [5]. Here, we apply these spectral criteria to reflectance spectra of terrestrial opals and to CRISM data in order to evaluate their validity on Martian data and to better understand the major geological processes that formed hydrated silica on Mars.

Data and Methods: IR reflectance spectra have been aquired on terrestrial opals for which geological origins are well established. For the investigation of opal on Mars, we use CRISM data over several sites where opals are present and formation conditions have been proposed in the literature on the basis of geomorphological criteria and the present associated minerals. I/F-converted CRISM images are corrected from atmospheric gas absorptions by the scaled volcano-scan method [6]. Extraction of opal CRISM spectra have been conducted using the processing tools specified in [7]. Opal is identified in CRISM data by its main spectral absorption bands at 1.4, 1.9 and 2.2 µm related to its water content [3, 4, 5, 8] (Fig. 1A). These spectral analyses have been correlated with HiRISE and CTX images in order to assess the geomorphological settings of these opal deposits.

All opal spectra are smoothed with the Savitsky-Golay method [9]. Continuum of smoothed spectra are removed by using the Segmented-Upper-Hull Method [10]. Each absorption band is fitted using gaussian functions depending on spectral absorptions produced by the presence of isolated or H-bonded silanols and water molecules in opal [3, 4, 5, 8]. Eventually, criteria calculations are conducted on the simulated spectra after gaussian deconvolutions.

The criterion used in this work to discriminate supergene from hydrothermal opals is named the concavity ratio criterion, or CRC [5]. For an asymmetric absorption band, it is calculated as the ratio between the true band-depth of the high-wavelength side and the virtual band-depth of it that is interpolated onto a linear continuum connected to the reflectance minimum and a low-frequency anchor point (Fig 1B). This operation does permit us to estimate the shape of an asymmetric feature. The more convex the high-wavelength side is, the higher and closer to 1 the CRC is. Hydrothermal opals show, regardless of their structure (opal-A/CT), more convex bands than supergene opals, and hence have higher CRC values (Fig 1A).

Bias in the data and limitations may affect our results. The shape of the 1.4 µm feature is modified by opal dehydration [3, 4]. The 1.9 µm feature may have residual atmospheric CO_2 absorptions that enlarge high-wavelength side of the 1.9 µm band even if opal encountered dehydration, and therefore results in a hydrothermal-like signature.

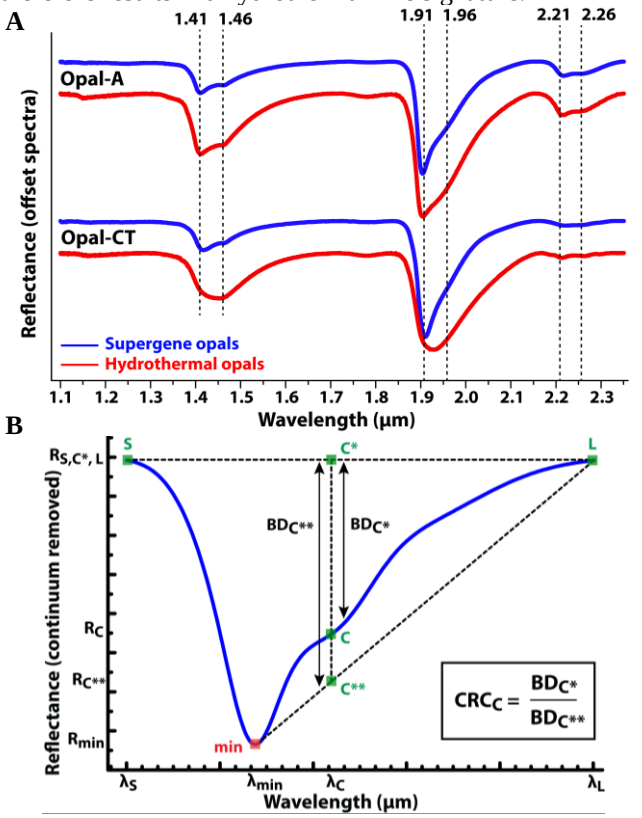

Fig 1. A) Reflectance spectra of terrestrial opals, dotted vertical lines indicate positions of main classical opal absorptions. **B)** Diagram illustrating CRC calculation of an asymmetric absorption band.

Results: Criteria applied on terrestrial opals show that the 1.4 µm band minimum position allow to distinguish opal-A from opal-CT having a threshold at ~1.415 µm between the two opal types (Fig 2). Additionaly, $CRC_{1.4}$ values enable to discern between supergene and hydrothermal

opals, with threshold $CRC_{1.4}$ ~0.96 (Fig 2). These criteria applied on the 1.9 µm band show similar results with a distinction between opal-A and opal-CT at ~1.908 µm, and a hydrothermal/supergene-distinction at $CRC_{1.9}$ ~0.81. The 2.2 µm band, affected by Si-OH silanol and Si-O-Si siloxane contributions, does not permit to distinguish neither the type of opals nor their formation processes. These results are in agreement of previous studies conducted on IR transmission spectra of the same terrestrial opals [5].

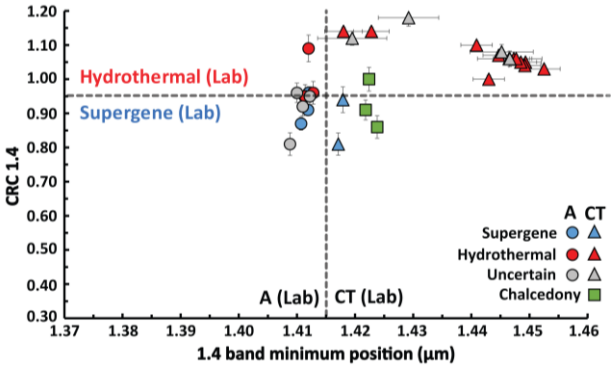

Fig 2. Plot showing the 1.4 band minimum position vs. $CRC_{1.4}$ calculations for terrestrial opals.

Calculated criteria on the 2.2 µm band of the Martian data does not seem to distinguish opal origin and/or crystallinity. Martian opals, which are putative to be hydrothermal in origin in the literature, have higher $CRC_{1.4}$ values than putative supergene opals. The $CRC_{1.4}$ threshold that separates supergene and hydrothermal Martian sites is shifted at a lower value than the terrestrial $CRC_{1.4}$ threshold. Moreover, these criteria suggest two clusters: opal-bearing rocky outcrops with low $CRC_{1.4}$ values and minima consistent with opal-A, and opal-bearing aeolian deposits with high $CRC_{1.4}$ values and minima consistent with opal-CT (Fig 3).

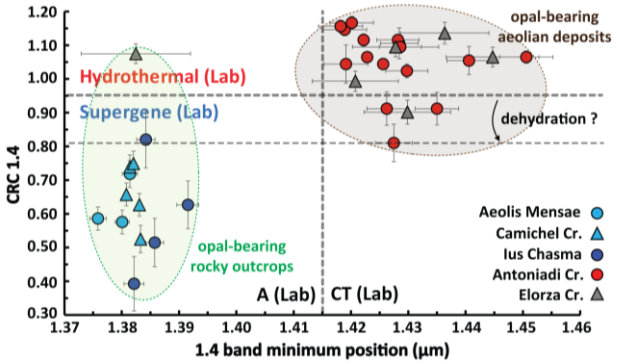

Fig 3. Plot showing the 1.4 band minimum position vs. $CRC_{1.4}$ calculations for the Martian CRISM data.

Overall, similar results are obtained on the 1.9 µm band, even though there are differences with the 1.4 µm feature. The $CRC_{1.9}$ threshold separating hydrothermal and supergene opals on Mars is not shifted compared to the threshold observed on terrestrial opals.

Discussion: CRC calculations applied to CRISM data are in rather good agreement with the formation processes and silica habitus proposed in the literature.

Opals of aeolian deposits are more crystalline than those of rocky outcrops (minima at high wavelengths) (Fig. 4). Opal-bearing aeolian deposits are mostly located around central peaks of impact craters. Therefore, impact-induced hydrothermalism is likely at the origin of opal formation in these aeolian deposits which is consistent with their high-CRC values. Alternatively, certain authors suggest that this silica is more mature (high crystallinity) because of its granular texture that facilitate interactions with surface water [4, 11].

Opals in rocky outcrops correspond to amorphous silica and/or dehydrated opals (minima shifted at low wavelengths) (Fig. 4). Their low-CRC values are consistent with supergene opals, and hence for significant surface-atmosphere interactions.

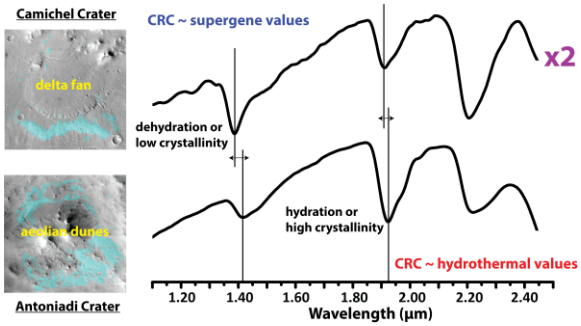

Fig 4. Spectra of Martian opals in two different geomorphological settings (opal-bearing rocky outcrops on top and opal-bearing aeolian deposits at bottom).

Conclusions: Spectral criteria based on band minimum positions and concavity (CRC) can be applied to CRISM data in order to investigate the origin and crystallinity of opals on Mars especially in regions where geomorphological contexts are ambiguous. Our study shows two major opal groups on Mars: opal-bearing aeolian deposits consistent with opal-CT, mostly of hydrothermal origin; and opal-bearing rocky outcrops associated to opal-A and/or dehydrated opals mostly of supergene origin. Further investigation will aim to better constrain the nature of these opal groups and the implications for Early Mars conditions.

References: [1] Carter et al. (2013) *JGR, 118*, 1–28. [2] Ehlmann and Edwards (2014) *Annu. Rev. Earth Planet. Sci., 42*, 291-315. [3] Rice et al. (2013) *Icarus, 223*, 499-533. [4] Sun et al. (2017) *LPSC48*, #1715. [5] Chauviré et al. (2017) *Eur. J. Mineral., 29*, 409-421. [6] McGuire et al. (2009) *Planet. Space Sci., 57*, 809-815. [7] Carter et al. (2013) *Planet. Space Sci., 76*, 53-67. [8] Langer and Flörke (1974) *Fortschr. Miner., 52*, 17-51. [9] Savitzky and Golay (1964) *Anal. Chem., 36*, 1627-1639. [10] Clark et al. (1987) *Workshop JPL, 87-30*, 138-142. [11] Tosca and Knoll (2009) *Earth Planet. Sci. Lett., 286*, 379-386.

Acknowledgments: We acknowledge the support from the Agence Nationale de la Rechreche (ANR, France) under the contract ANR-16-CE31-0012 entitled Mars-Prime, and the Centre National de la Recherche Scientifique (CNRS, France).